

# TANDEM SUBMERGED CYLINDERS EACH SUBJECT TO ZERO DRAG

E.O. Tuck and D.C. Scullen

Applied Mathematics Department  
The University of Adelaide

Revised June 1997.

## Summary

Two identical circular cylinders are submerged to the same depth in tandem in a stream. There are separation distances between the cylinder centres such that the combination makes no downstream waves, and hence is subject to zero net wave drag. In general there is then a nonzero equal and opposite horizontal force on each cylinder. However, there are special depths of submergence such that this interaction force between the cylinders also vanishes, and hence each cylinder is separately free of horizontal force. The parameter range for this phenomenon is explored both by linear theory for cylinders of small radius, and by a fully-nonlinear computer program. For example, a configuration with a separation distance of approximately one half-wavelength gives zero force on each cylinder when the depth of submergence is approximately three-quarters of the separation distance.

## 1. Introduction

If two similar bluff bodies are placed in a stream  $U$  in close tandem, there are grounds for anticipating a repulsive force of interaction between the bodies. That is, the trailing body exerts a thrust on the leading body. For example, if the trailing body were alone, it would have a stagnation zone ahead of it and hence a positive pressure gradient in the streamwise direction. If one then placed another body in that zone, one would expect this pressure gradient to push the new body forward. In any case, the combination may be expected to yield a relatively low velocity in the space between them, and hence a higher pressure there than that acting on the front of the leader. The resulting pressure difference would create a net forward force on the leader. This “induced-buoyancy” force allows dolphins to coast freely immediately in front of the bow of fast-moving ships, and has nothing to do with wave generation, gravity  $g$ , or the presence of a free surface (Newman 1975).

On the other hand, dolphins (and humans!) can also surf on the free-surface waves behind a ship. And baby ducks do seem to benefit from swimming in close formation behind their mother. So it may also be possible for there to be a force of attraction between two bodies in tandem near a free surface, and we shall show examples of this for submerged cylinders. This is essentially a gravity-wave phenomenon, and it is not hard to see that wave effects will tend to lead to a drag force on the leading body, not a thrust. For example, in the limit of large (many wavelengths) separation, the leader will not detect the presence of the trailer, and will then be subject to the same wave resistance or positive drag as if it was

alone.

For submerged bodies, each of these two distinct and opposite phenomena plays a role, and the net effect on the leading body is the sum of local thrust and wave drag forces. Hence it is possible for these forces to cancel each other out, and for the leading body to be subject to zero force. To achieve this, it is only necessary to adjust the depth of submergence so that the wave drag, which is very strongly dependent on depth, is equal and opposite to the local thrust, which is essentially the same for all depths. This is in principle possible for any reasonably shaped pair of bodies at any (not too small) separation distance, though most easily realisable for similar or identical bodies. It holds both in two and three dimensions; for example, Xu (1996) has shown that the leader of two tandem spheres can have zero (or negative) drag in some circumstances.

In two-dimensional flow, if we combine two linear wave-makers with closely similar properties, it is possible to use destructive interference between phase-shifted separate wave patterns to cancel the combined far-downstream waves. For example, this can be done by a combination of a thickness and lifting effects for submerged airfoil-like bodies (Tuck and Tulin 1992), and for a single circular cylinder with appropriately chosen circulation (Scullen and Tuck 1995). Even more familiar examples occur for single bodies or pressure distributions of finite extent (Lamb 1932 p. 404, Vanden-Broeck and Tuck 1985), or finite-length bumps on the bottom of water of finite depth (Forbes 1982), where cancellation occurs essentially via destructive interference between out-of-phase bow and stern-generated waves.

In the present case of two separate bodies in tandem, such cancellation can occur for appropriate separation distances, if the bodies are identical and at the same depth of submergence. In that case, there will be zero net drag on the combination. This is known to be an exact result in the linear case, and we shall show that to the accuracy of our computations it also happens for nonlinear disturbances. Thus according to linear water-wave theory with small-amplitude sinusoidal waves of wavelength  $2\pi U^2/g$  (Newman 1977, p. 270), exact wave cancellation occurs when the separation  $\ell$  between identical wave-making bodies is an odd multiple of a half-wavelength, namely  $\ell = (2n + 1)\pi U^2/g$ ,  $n = 0, 1, 2, \dots$ . Linear theory is valid for bodies that are sufficiently small or sufficiently deeply submerged. Otherwise the waves made are nonlinear and non-sinusoidal, and there is no guarantee that exact and complete cancellation can be expected, nor any prior information about the discrete separations at which such cancellations might occur. Schwartz (1981) and Forbes (1982) did however give strong numerical evidence for exact cancellation of nonlinear waves made by pressure distributions and bottom bumps respectively, and we present similar evidence here for tandem submerged cylinders.

It is in any case clear that depth of submergence tends to control the force on the leading body, while separation between the bodies controls the net force on the combination. It is therefore possible that by simultaneous adjustment of both distances we may be able to eliminate both forces, and hence to achieve a situation where each body is subject to zero force. We expect a discrete set of such configurations, parametrised by an integer  $n$  as above. Given the shape and size of the identical bodies, for each  $n = 0, 1, 2, \dots$  there will be a unique depth  $h$  and a unique separation  $\ell$  (each scaled with  $U^2/g$ ) for zero force. Hence the depth/separation ratio  $h/\ell$  of the configuration is uniquely determined for each  $n$ . The  $n = 0$  configuration has the smallest (half-wavelength) separation, and hence the largest local thrust. Hence it needs the largest wave for cancellation purposes, so has the least depth of submergence.

As a specific example, let us specialise to a pair of identical submerged circular cylinders of radius  $a$ , with their centres at the same depth  $h$ , but separated horizontally by a distance  $\ell$ . Then linear theory applies when  $a$  is sufficiently small relative to all other length scales, and suggests that the zero-force configuration is independent of  $a$ . The force on each cylinder is proportional to  $a^4$  in this linear theory, and a formula for this force is derived here. Although this formula is somewhat complicated, involving the complex exponential integral function, a simple far-field expansion appears to be of adequate accuracy. The linear conclusion is that, with  $\ell = (2n+1)\pi U^2/g$  as discussed above, the zero-force configurations have  $h/\ell = 0.759, 0.422, 0.294, \dots$  for  $n = 0, 1, 2, \dots$

The linear results are then confirmed by use of a computer program (Scullen and Tuck 1995) which solves two-dimensional potential flows for submerged bodies of any shape. The present problem of two submerged tandem circular cylinders is solved to (in principle) arbitrary precision by this program, with the correct impermeability boundary condition on both cylinders, and the full nonlinear free-surface conditions. When that program is run at small  $a$ , say of the order of a tenth of  $U^2/g$ , the asymptotic small- $a$  results are reproduced. The program then enables determination of the effect of nonlinearity, by increasing  $a$ , and results are obtained in a range up to  $a$  values comparable to  $U^2/g$ ,  $h$  and  $\ell$ .

The conclusion is that zero force on either cylinder demands larger submergences and separations when nonlinearity is important. There is still a discrete set of configurations yielding (to the accuracy of our computations) essentially zero force simultaneously on both cylinders, the most important member ( $n = 0$ ) of which still has a depth of about three-quarters of the separation.

For every submergence yielding non-breaking waves, we can find separations such that the configuration makes no waves far downstream, to within the accuracy of our program. The corresponding flow is fore-aft symmetric, with a large trough between the cylinders and small crests above them. If one compares configurations with separations either just less than or just greater than a non-wavemaking value, there is a clear change of phase in the wave produced far downstream. In general, for such non-wavemaking configurations, there is an equal and opposite force on each of the cylinders separately. However, for each cylinder radius, there is a discrete set of submergences, as described above, for which this separate force vanishes.

For very large cylinders, if one further increases or decreases the separation from a non-wavemaking value, the wave amplitude rises very steeply and the waves become noticeably non-sinusoidal. For some sufficiently large cylinder radii, computation is feasible using our present program only in a very narrow range of separations close to the non-wavemaking value. Solutions with non-breaking waves may in fact only exist in this narrow range for such large disturbances.

## 2. Linear Theory

Consider the complex potential

$$f(z) = Uz + Ua^2 [G'(z) + G'(z - \ell)] \quad (1)$$

where  $G(z)$  is the potential for a source beneath a free surface, such that  $G(z) - \log z$  is analytic near  $z = 0$ ; thus  $G'(z)$  is a dipole potential, behaving like  $1/z$  for small  $z$ . The

equilibrium free surface is  $y = h$ , on which  $G$  satisfies the linearized free-surface condition

$$\Re[U^2 G''(z) + igG'(z)] = 0 \quad (2)$$

Specifically (Havelock 1926, Wehausen and Laitone 1960, p. 489, Tuck 1965)

$$G(z) = \log z + F(2\kappa h + i\kappa z) \quad (3)$$

where  $\kappa = g/U^2$  and

$$F(v) = \log v - 2e^{-v} Ei^-(v), \quad (4)$$

with  $Ei^-$  an exponential integral function (Jahnke and Emde 1945, p. 1).

The velocity potential (1) thus describes a flow about a pair of submerged dipoles, separated by a distance  $\ell$ . It is not the exact solution for flow over any actual body or combination of bodies; indeed (Tuck 1965) it is unlikely even to generate exactly any closed stream surface. However, the flow near  $z = 0$  is dominated by the local dipole, and thus

$$f(z) \approx Uz + Ua^2/z + \text{constant} \quad (5)$$

which is the exact solution for flow over a circular cylinder of radius  $a$  at the origin. Similarly, if we consider small values of  $z - \ell$ , we see that the flow approaches that for a circle of radius  $a$  at that point. Hence for sufficiently small  $a$  the potential above approximates that for flow over a pair of circles of radius  $a$  separated by a distance  $\ell$  and submerged to a depth  $h$ .

In order to compute the force on the leading circle at  $z = 0$ , we must continue the expansion begun by (5) to several more terms, and in particular find the coefficient of  $1/z$  in the Laurent series of the squared velocity  $f'(z)^2$ . Namely

$$f'(z)^2 = \sum_{j=-4}^{\infty} C_j z^j \quad (6)$$

where

$$C_{-1} = -2U^2 a^4 [(i\kappa)^3 F'''(2H) + G'''(-L)] \quad (7)$$

with  $L = \kappa\ell$  and  $H = \kappa h$ . Then Blasius formula (Milne-Thomson 1968, p. 168)

$$X - iY = \frac{1}{2} i\rho \int [f'(z)^2] dz = -\pi\rho C_{-1} \quad (8)$$

gives the drag  $X$  and lift  $Y$  on the body. In particular, the drag  $D = X$  on the leading circle is

$$D = -\pi\rho \Re C_{-1} \quad (9)$$

$$= 2\pi\rho U^2 a^4 \Re [(i\kappa)^3 F'''(2H) + G'''(-L)] \quad (10)$$

$$= 4\pi^2 \rho U^2 a^4 \kappa^3 e^{-2H} + 2\pi\rho U^2 a^4 \Re G'''(-L) \quad (11)$$

It is convenient to define a drag coefficient

$$C_D = \frac{D}{4\pi\rho U^2 a^4 \kappa^3} \quad (12)$$

for which we have found finally the linearised result

$$C_D = \pi e^{-2H} - L^{-3} + \Im \left[ e^{-v} Ei^{-}(v) - v^{-1} - v^{-2} - v^{-3} \right] \quad (13)$$

where  $v = 2H - iL$ .

In order to evaluate this force, it is in general necessary to compute values of the exponential integral  $Ei^{-}(v)$  with complex argument  $v$ , which can be done reasonably efficiently for moderate values of the argument  $v$  by summing its Taylor series (Jahnke and Emde 1945, p. 2). However, for the relatively-large  $H, L$  values of prime interest here, a large- $v$  asymptotic expansion is often sufficient, in which only the two leading terms of (13) need be retained, namely

$$C_D = \pi e^{-2H} - L^{-3} . \quad (14)$$

The physical interpretation of this formula is as follows. The first term is just the wave resistance of the leading circle in the absence of the trailing circle, and thus is independent of the separation  $L$ . The second term is the main local thrust from the interaction between the two circles. Note that this term is independent of  $H$ , and indeed can be found by ignoring the free surface, and just combining a stream with two simple dipoles in an infinite fluid. This simple approximate formula thus captures the drag and thrust force components due to far-field waves and local overpressures respectively. The only change if one reverts to the full linear formula (13) is to give a slightly more accurate estimate of the local thrust term.

The force on the trailing body can be found similarly. In fact it follows simply by replacing  $L$  by  $-L$  in (13). This is a physically significant change, since then there are non-local (wave) effects from  $G'''(L)$  representing the fact that the trailing body lies in the wave wake of the leading body, and the far-field approximation is not the same as would follow simply by replacing  $L$  by  $-L$  in (14). Specifically, the large- $v$  expansion for the drag on the trailing body then becomes

$$C_D = \pi e^{-2H} (1 + 2 \cos L) + L^{-3} . \quad (15)$$

For large  $L$  this oscillates between a drag of three times the wave drag of a single circle and a thrust equal and opposite to that drag.

The total drag on the combination is the sum of the above forces on the two circles, namely (as an exact linear result, without any far-field approximation)

$$C_D = 2\pi e^{-2H} (1 + \cos L) \quad (16)$$

which vanishes when  $L$  is an odd multiple of  $\pi$ , as expected.

According to the approximate formula (14), the force on the leading cylinder vanishes when

$$H = \frac{1}{2} \log \left[ \pi L^3 \right] \quad (17)$$

and a corresponding graph of  $H$  versus  $L$  is shown as the chain-dotted curve in Figure 1, labelled “ $A = 0$  (approx.)”. On the other hand, if we set  $C_D = 0$  in the full linear formula (13), and for each value of  $L$  use Newton iteration to find the corresponding value of  $H$ , this gives the dashed curve labelled “ $A = 0$  (exact)” of Figure 1, the difference

from the chain-dotted curve being only a few percent in the range shown. In particular, for the lowest-order wave-cancelling separation  $L = \pi$ , the approximate formula gives  $H = \log \pi^2 = 2.289$  whereas the full linear result has  $H = 2.385$ , the latter corresponding to a configuration aspect ratio of  $h/\ell = 0.7592$ . The second wave-cancellation mode  $L = 3\pi$  is such that the far-field approximation  $H = 3.937$  is even closer to the full linear result  $H = 3.974$  ( $h/\ell = 0.4216$ ), and as we move to higher modes, the separations and depths increase further. In practice the main interest is in the lowest mode.

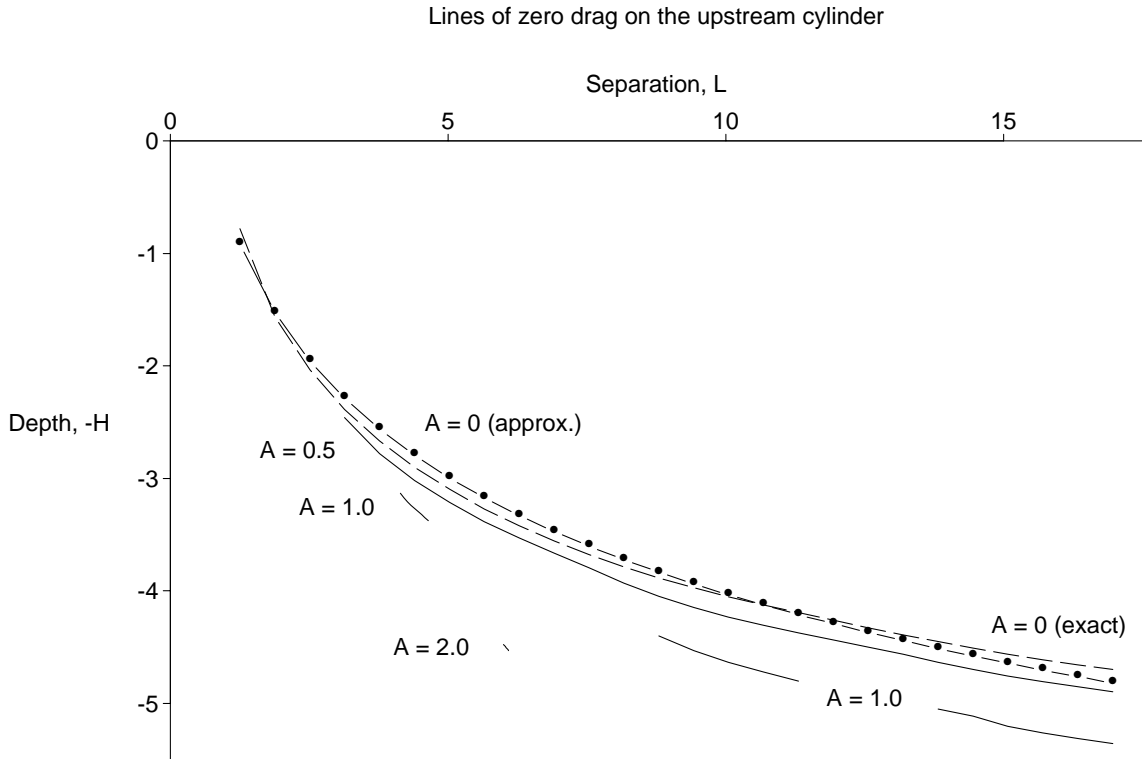


Figure 1: Relationship between nondimensional depth  $H$  and separation  $L$  yielding zero horizontal force on the leading cylinder, for various nondimensional radii  $A$ . The chain-dotted curve is a far-field approximation (17) to the linear ( $A = 0$ ) theory, for which the exact results are shown as the dashed curve.

### 3. Exact Computations

A program has recently been developed (Scullen and Tuck 1995) that enables solution of potential flows about submerged bodies of any shape, even at submergences such that the waves made are highly nonlinear. The (known) body surface and (unknown) free surface are each represented by a collection of discrete points, while discrete sources located outside of the flow domain (inside the body or above the free surface) are used to generate the velocity potential for the flow, with strengths to be determined.

For each choice of the number  $n$  of specified boundary points (and hence of unknowns to be solved for), all boundary conditions are satisfied at these collocation points to as fine an accuracy as desired. The iteration scheme, in which approximations to the free

surface and its associated velocity potential are successively refined at a fixed value of  $n$ , has been carefully designed so that a quadratic rate of convergence is achieved at the collocation points. Once such convergence has been achieved, the residual error, e.g. at points intermediate between collocation points and in the force computations, then depends on the value of  $n$ , and we have found that approximately 6 figure accuracy is achieved for  $n$  values of the order of 1000.

The benefit of using singularities external to the fluid domain, as opposed to locations on its boundary, is that a smoother representation of the potential can be achieved along the boundaries, which in turn leads to a more accurate solution for a given  $n$ . Discrete rather than distributed sources prove to be suitable for representing bodies without sharp corners, and have the additional benefit that derivatives up to third order (which are required by the method) are simple to evaluate. The body forces are determined by application of the Lagally theorem (Milne-Thomson 1968) which relies solely upon knowledge of the locations of the sources and their strengths, and avoids the need for numerical integration of pressure over the surface of the body.

The program has previously been applied to (single) submerged circular cylinders both with and without circulation (Scullen and Tuck 1995) and to submerged spheroids in three dimensions (Scullen 1996).

The present extension to two submerged tandem cylinders presents no additional difficulties. For a given choice of nondimensionalised cylinder radius  $A = \kappa a$  and separation  $L$ , results are first obtained for the drag on the first cylinder as a function of depth  $H$ . When the program was run for cylinders of small nondimensional radius  $A$ , the results were close to those given by the linear theory. We then use the secant method to search for the depths  $H$  at which the computed force on the leading body vanishes. The results for  $H$  as a function of  $L$  are in approximately 4-figure agreement with the linear theory at  $A = 0.01$ , and still in better than 2-figure agreement at  $A = 0.1$ . Thus for all  $A \leq 0.1$ , the (dashed) curve labeled “ $A = 0$  (exact)” of Figure 1 was reproduced to within plotting accuracy by the nonlinear computations.

At higher values of  $A$ , some differences appear. Large cylinders make large waves, and the rate of increase in wave-making (at fixed depth) is greater than the rate at which the thrust due to local overpressure increases with the size of the cylinders. Hence larger cylinders need to be submerged deeper in order to cancel the force on the leading cylinder. Figure 1 shows the required depths for various  $A$  values.

Note that the nonlinear computations are incomplete. For example, gaps in the curve for  $A = 1$  are indications that the program has failed to converge because of the large amplitude of the waves produced. These waves may indeed have become so steep that there may not even exist solutions in some parameter ranges, the waves having broken at their crests in practice. For the most nonlinear case so far examined, namely  $A = 2$ , the parameter range where solutions are found is so narrow that on the scale of Figure 1, it appears as just a very short line segment near  $L = 6$ , but nevertheless contains useful results.

Meanwhile, the program also confirms for small cylinders the set of nondimensional separations  $L = \pi, 3\pi, \dots$  that cancel the near-linear waves made by the combination. For larger cylinders, there is no guarantee that exact wave cancellation occurs, since there is

no superposition principle for the nonlinear waves then produced. However, to the accuracy of our computations, it does appear that there exists a discrete set of separations yielding exactly zero downstream wave amplitude and hence exactly zero wave drag on the combination. The flow at these separations appears to be fore-aft symmetric, which is indirect confirmation that even in the fully nonlinear case there are flows without waves far downstream.

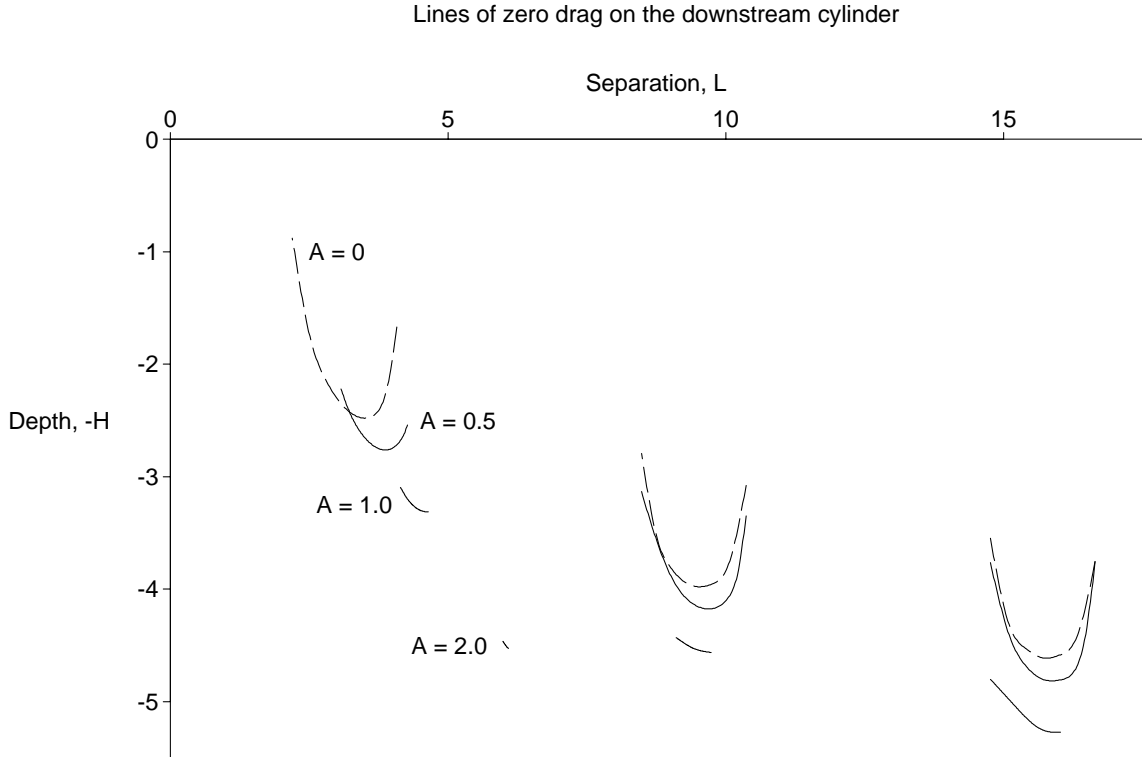


Figure 2: Same as Figure 1, but for zero force on the trailing cylinder.

The wave-cancelling separation values of  $L$  now depend on  $H$  as well as  $A$ , whereas in the linear theory they are independent of both. Because the corresponding total drag is non-negative, a parameter search for its near-zero minima is a difficult numerical task. Instead, it is somewhat more convenient to proceed indirectly, as follows. Figure 2, like Figure 1, contains graphs of depth  $H$  versus separation  $L$  for various fixed values of cylinder radius  $A$ , but now these are depths at which the force on the trailing rather than the leading cylinder vanishes. Configurations with zero force on either cylinder separately are easier to obtain than those for zero total force, since they involve zero-crossings rather than zero minima. Again the results for small radius  $A$  agree with the linear theory. Again, for large  $A$ , the nonlinear curves are incomplete, but some low-wave results are obtained even for  $A$  as high as 2.

For any given cylinder radius  $A$ , a configuration with zero force on both cylinders (and hence necessarily with no waves) would be obtained wherever the curves of Figures 1 and 2 meet. In the linear theory, these curves touch exactly at  $L = \pi, 3\pi, \dots$ , as expected. The nonlinear program indicates that the curves still appear to touch each other, but at larger

values of  $L$ , which depend on the radius  $A$ .

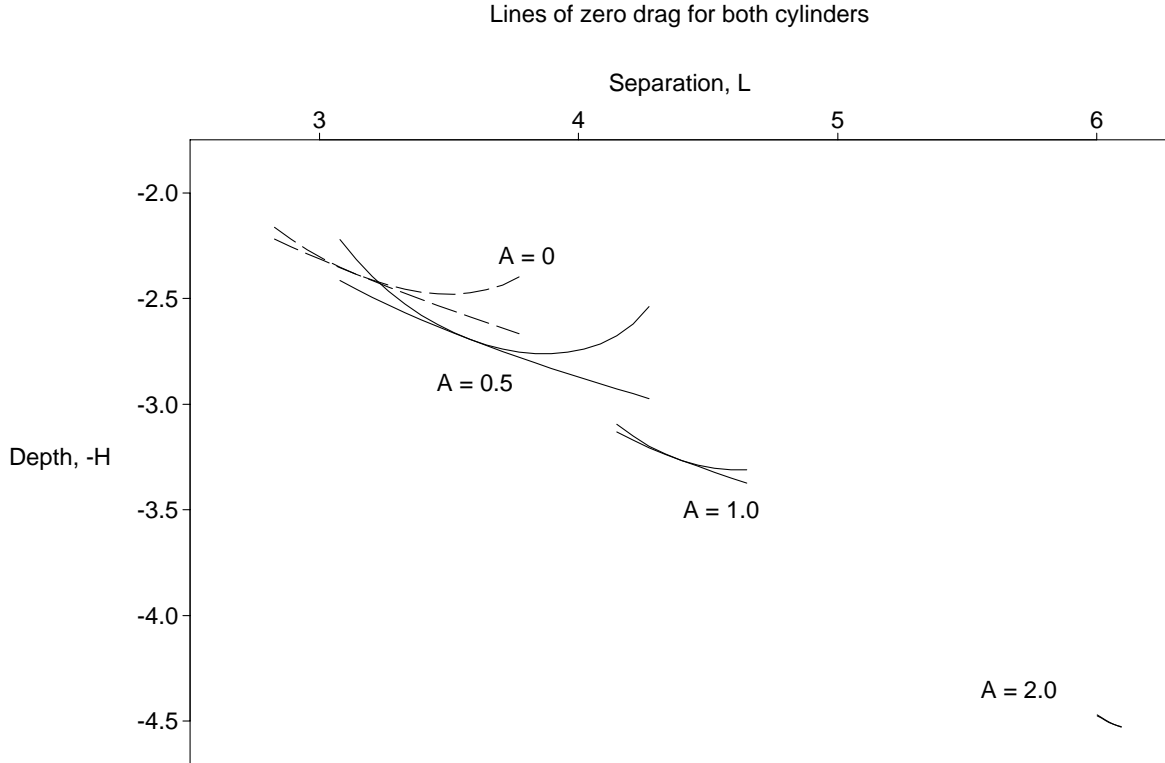


Figure 3: Combination of curves of Figures 1 and 2, in the range of the principal mode  $n = 0$ .

In particular, Figure 3 shows an expanded view of a combination of the curves of Figures 1 and 2, in the neighbourhood of the principal mode  $n = 0$  where  $L = \pi$  in linear theory. On the scale of this Figure, touching of these two curves appears to occur up to  $A = 1$ , and also at  $A = 2$ , even though for that radius only a very narrow range of separations from  $L = 6.000$  to  $L = 6.095$  allows convergence of our computer program, and the two “curves” are indistinguishable short line segments. The depths and separations required for zero force on both cylinders both increase quite dramatically with nonlinearity, almost doubling the linear values at  $A = 2$ , but their ratio stays almost constant at about 0.75 for the  $n = 0$  mode.

Figure 4 is a sample of free-surface shapes for cylinders with  $A = 1$ . The curves are for a narrow range of values of  $L$  as in Figure 3, centered about the principal zero-force configuration. At each value of  $L$ , the depth  $H$  has been chosen as in Figure 1 so that there is zero force on the leading cylinder. The least wave amplitude (and hence the least force on the combination) appears to occur at  $L = 4.369$  with  $H = 3.254$ . This minimum force is essentially zero to within the order of error of our program, typically say  $10^{-7}$  for the drag coefficient  $C_D$  defined in equation (12), which takes values of the order of unity otherwise.

In Figure 4, note the nonlinearity, with sharp crests and broad troughs, of the highest

Free-surface shapes for  $A=1.0$

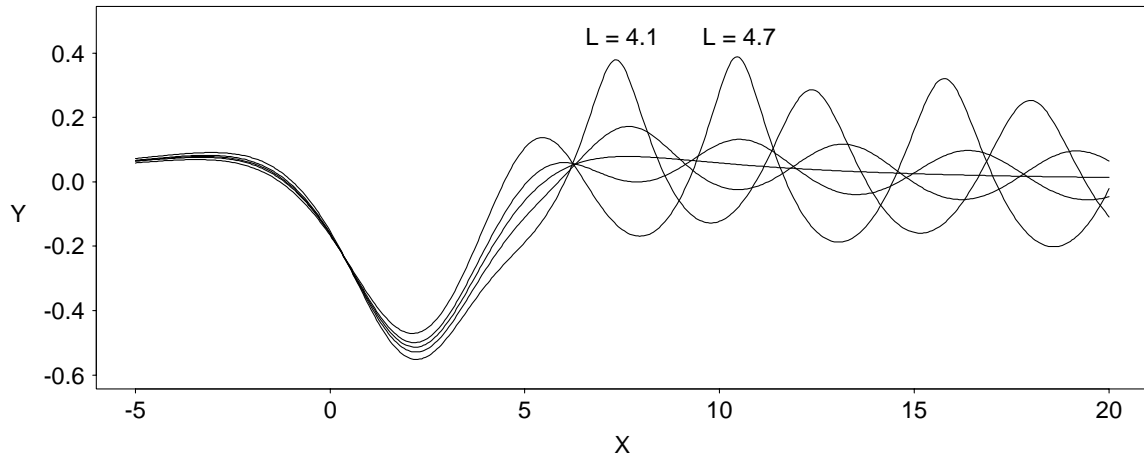


Figure 4: Free-surface waves behind cylinders with  $A = 1$ , for  $L = 4.1, 4.27, 4.37, 4.46$  and  $4.7$ , all such that there is zero force on the leading cylinder.

waves shown, at  $L = 4.1$  and  $L = 4.7$ . The rapid growth of these waves as  $L$  departs from the near-zero wave state is a signal for eventual failure of our program to converge, and likely non-existence of non-breaking solutions.

It is also notable in Figure 4 that the waves for  $L = 4.27$  and  $L = 4.46$  are almost out of phase with each other, indicating that a zero-wave state is likely somewhere between them. Indeed, it is possible to find such zero-wave solutions for every value of  $L$  by suitable adjustment of  $H$ . The point of the present study is that within this family is a unique member having an essentially zero value for the force on each cylinder separately, and that member has  $L = 4.369, H = 3.254$  at  $A = 1$ .

Similarly, for the even larger cylinders with  $A = 2$ , the zero-force member has  $L = 6.06, H = 4.51$ . Figure 5 indicates the free surface near the cylinders for that member. The flow appears to be fore-aft symmetric. Note the large trough between the cylinders, which has a depth that is more than double the height at which stagnation of the flow would occur. This tandem cylinder configuration is already quite a large local free-surface disturber, but nevertheless one which leaves no trailing wave pattern far downstream, and has zero horizontal force on each cylinder.

## References

- FORBES, L.K. 1982 Nonlinear drag-free flow over a submerged elliptical body. *J. Engng Maths* **16**, 171-180.
- HAVELOCK, T.H. 1926 The method of images in some problems of surface waves. *Proc. Roy. Soc. Lond. Ser. A* **115**, 268.
- JAHNKE, E. & EMDE, F. 1945 *Tables of Functions*, 4th edn. New York: Dover.
- LAMB, H. 1932 *Hydrodynamics*, 6th edn. New York: Dover.

Approximately symmetric solution for  $A=2.0$

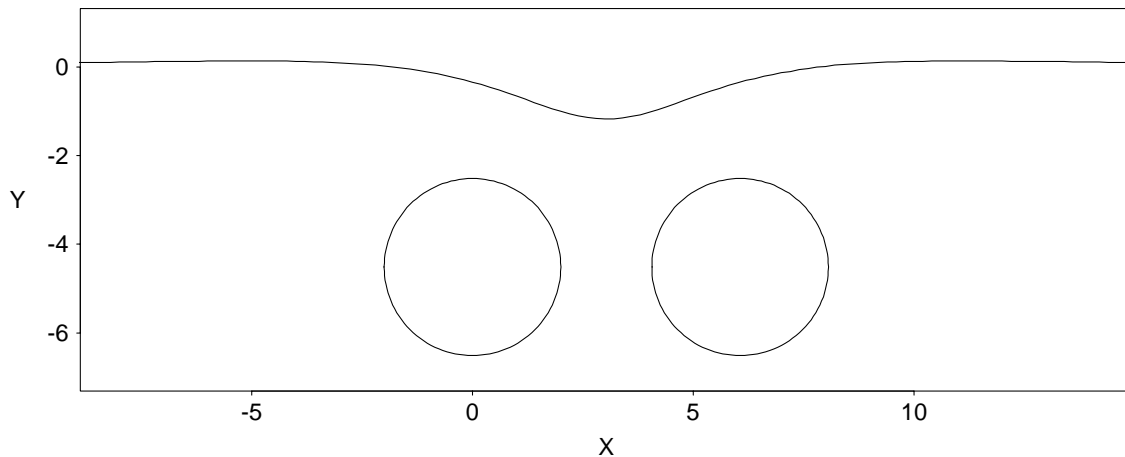


Figure 5: Free surface near cylinders with  $A = 2$ ,  $L = 6.06$  and  $H = 4.51$ .

MILNE-THOMSON, L.M. 1968 *Theoretical Hydrodynamics*, 5th edn. New York: MacMillan.

NEWMAN, J.N. 1975 Swimming of slender fish in a non-uniform velocity field. *J. Austral. Math. Soc. Ser. B* **19**, 95-111.

NEWMAN, J.N. 1977 *Marine Hydrodynamics*. Cambridge, Mass.: MIT Press.

SCHWARTZ, L.M. 1981 Nonlinear solution for an applied overpressure on a moving stream. *J. Eng Math.* **15**, 147-156.

SCULLEN, D.C. & TUCK, E.O. 1995 Nonlinear free-surface flow computations for submerged cylinders. *J. Ship Res.* **39**, 185-193.

SCULLEN, D.C. 1996 Three-dimensional steady state nonlinear free-surface flow computation. *Gazette Austral. Math. Soc.* **23**, 80-84.

TUCK, E.O. 1965 The effect of non-linearity at the free surface on flow past a submerged cylinder. *J. Fluid Mech.* **22**, 401-414.

TUCK, E.O. & TULIN, M.P. 1992 Submerged bodies that do not generate waves. *7th Int. Workshop on Water Waves and Floating Bodies*. Proceedings ed. R. Cointe, Bassin d'Essais des Carenes, Val de Reuil, France, pp. 275-279.

TUCK, E.O. & VANDEN-BROECK, J.-M. 1985 Waveless free-surface pressure distributions. *J. Ship Res.* **27**, 151-158.

WEHAUSEN, J.V. & LAITONE, E.V. 1960 Surface waves. *Handbuch der Physik*, **9** Ed. S. Flugge, Berlin: Springer-Verlag.

XU, G.X. 1996 Wavemaking resistance of a group of submerged spheres. *J. Ship Res.* **40**, 1-10.